


Article

Feasibility of Eco-Friendly Binary and Ternary Blended Binders Made of Fly-Ash and Oil-Refinery Spent Catalyst in Ready-Mixed Concrete Production

Carla Costa ^{1,*}  and José Carlos Marques ²¹ ISEL—Instituto Superior de Engenharia de Lisboa, Instituto Politécnico de Lisboa, 1959-007 Lisbon, Portugal² Betão Liz S.A., InterCement/Cimpor Group, 1250-009 Lisbon, Portugal; JCMarques@intercement.com

* Correspondence: carlacosta@dec.isel.pt; Tel.: +351-910-885-900

Received: 20 July 2018; Accepted: 28 August 2018; Published: 3 September 2018



Abstract: Large-scale recycling of new industrial wastes or by-products in concrete has become a crucial issue for construction materials sustainability, with impact in the three pillars (environmental, social and economic), while still maintaining satisfactory, or improved, concrete performance. The main goal of the paper is to evaluate the technological feasibility of the partial, or total, replacement of fly-ashes (FA), widely used in ready-mixed concrete production, with spent equilibrium catalyst (ECat) from the oil-refinery industry. Three different concrete mixtures with binary binder blends of FA (33.3% by mass, used as reference) and of ECat (16.7% and 33.3%), as well as a concrete mixture with a ternary binder blend with FA and ECat (16.7%, of each) were tested regarding their mechanical properties and durability. Generically, in comparison with commercial concrete (i) 16.7% ECat binary blended concrete revealed improved mechanical strength and durability; (ii) ternary FA-ECat blended binder concrete presented similar properties; and (iii) 33% ECat binary blended concrete has a lower performance. The engineering performance of all ECat concretes meet both the international standards and the reference durability indicators available in the scientific literature. Thus, ECat can be a constant supply for ready-mixed eco-concretes production, promoting synergetic waste recycling across industries.

Keywords: spent equilibrium catalyst (ECat); FCC catalyst; fly-ash; pozzolanic additions; ready-mixed concrete; industrial wastes recycling; blended binders; eco-friendly concrete; construction materials sustainability; circular economy

1. Introduction

Concrete is the most widely consumed construction material, exceeding 10 billion tons/year [1] worldwide, of which 165 million tons/year is in Europe [2]. In 2012, the cement and concrete industry directly generated 20 billion Euros in value and 384,000 jobs in the European Union [3]. Since this industry has a 2.8 multiplier factor in the overall economy [3], it has a major socio-economic impact.

In addition, the vast amount of natural resources and energy required by the concrete industry, [4] as well as its remarkable CO₂ emissions [5–7], make this sector indispensable towards a sustainable low carbon economy [8]. Most notably, concrete's ability to incorporate industrial wastes [9,10] provides a key opportunity to implement Circular Economy [8] whilst helping the European Union to achieve its targets set for waste recycling and resource efficiency [11], and also to tackle its Societal Challenge 'Climate action, environment, resource efficiency and raw materials' [12].

It is therefore natural that several industrial and agricultural wastes incorporated in cement-based materials have been under intense scrutiny by the scientific community [1,13–15]. Often, these investigations revealed that eco-concretes present improved performance including durability [15–17]. However,

among the vast number of surrogates investigated, only fly ash (FA) [10,18,19], ground-granulated blast-furnace slag [9,10,20], and silica fume [9,10] have already been consolidated in large-scale industrial application.

The uncertainty about the future availability of these surrogates, as well as the above-mentioned environmental, social, technological and economic reasons, encourage further knowledge transfer to industry, for which an industrial–academic collaboration is paramount. This framework permits that identified cement surrogates, besides complying with concrete standards and performance targets, also meet market demands, ensuring acceptance by end-users (designers, engineers, constructors and authorities).

The primary purpose of this study was to assess the technological feasibility of incorporating an equilibrium catalyst (ECat) waste, generated in Portuguese oil refinery, in the composition of a widely produced ready-mixed concrete, by Betão Liz company (Carnaxide, Portugal). The industrial concrete, used as a reference, is made with a binary binder of cement and FA pozzolan. ECat was investigated as partial or total FA substitute.

The ECat is a catalyst used in the fluid cracking catalytic units present in most of the oil refineries to optimize the crude oil refining process obtaining more valuable products, such as high-octane gasoline. When it loses enough catalytic activity, it is withdrawn from the process, thereby becoming a waste that is typically disposed of in landfills. More than 400 oil refineries worldwide use fluid cracking catalytic units [21] generating around 840 metric kt/year of spent ECat [22], of which 20% is in Europe [23]. Portuguese oil refinery industry withdraws 1.7 metric kt/year of ECat [24].

The ECat catalyst is a white-grey powder containing an aluminosilicate faujasite-type zeolite, an essentially amorphous alumina active matrix, clay and a binder. The crystalline structure of the zeolite is the main compound responsible for the ECat's very high specific surface ($> 100 \text{ m}^2/\text{g}$) [25].

Previous research has revealed that spent ECat is a cementitious material as it undergoes the pozzolanic reaction, which is the reaction with calcium hydroxide ($\text{Ca}(\text{OH})_2$) released during cement hydration. This reaction produces additional strength-providing reaction products, i.e., calcium aluminosilicate hydrates (C-A/S-H). The pozzolanic reactivity has been demonstrated monitoring the extension of the direct reaction of the ECat with $\text{Ca}(\text{OH})_2$ using titration methods, such as the Frattini test [26] and modified Chapelle test [27]. ECat's ability to undergo the pozzolanic reaction when it is incorporated in a cement-based matrix was also verified directly using thermo-gravimetric analysis (TGA) [28–30], X-ray diffraction [31] and Fourier transform infrared spectroscopy [32]. In addition, ECat pozzolanicity was verified indirectly using the strength activity index, i.e., the ratio between the compressive strength of a test sample with ECat incorporation in the binder by the compressive strength of a test sample without ECat [33,34].

The literature review also showed that when ECat partially replaced cement by up to 15–20% (by mass), it enhances both early and long-term strength of cement-based materials [34–36]. Moreover, it has also been shown that up to 10–15% of cement replacement by ECat has no adverse effect on the cement-based materials durability [35,37,38]. From a technological viewpoint, the ECat's main disadvantage as a pozzolanic material is the workability reduction that it promotes on the fresh state of cement-based materials, as its content in the binder increases due to its high surface area with water affinity [34,36,39].

The synergetic advantages of using ternary binders with ECat and FA has also been reported [29,40,41] revealing that FA counteracts the loss of workability in the fresh-state promoted by ECat; on the other hand, the ternary binder with ECat accelerates early hydration, as compared to the binary cement-FA binder, and it also improves the chloride ingress resistance.

Despite stated research results corroborating the advantages of ECat as cementitious material, as well as the significant amount of this waste availability worldwide, to the best of the authors' knowledge, this waste is not yet being used by the construction materials industry.

As such, an industrially-oriented investigation has been carried out. The ready-mixed concrete produced in plants of the Betão Liz company, made with a binary binder containing 33% (by mass) of

FA pozzolan, was used as reference. Two innovative concretes studied were made with binary binders of 16.7%, and 33% of ECat and one was made with a ternary blended binder of 16.7% of FA and 16.7% of ECat. Mechanical properties and concrete quality were evaluated through compressive strength and ultrasonic pulse velocity testing. Durability of concretes was estimated based on transport properties (capillary water absorption, chloride migration coefficient, and electrical resistivity).

2. Experimental Program Materials and Methods

2.1. Materials

The binding materials used were: commercial limestone Portland cement type CEM II/A-L 42.5R, according to European standard EN 197-1 produced by CIMPOR company (Alhandra, Portugal); fly ash (FA) from a thermoelectrical plant of the EDP company at Sines, Portugal; spent equilibrium catalyst (ECat) generated at the fluid cracking catalytic unit of the Portuguese oil-refinery company PETROGAL S.A. at Sines, Portugal.

CEM II/A-L containing up to 20% limestone reduces cement manufacture energy requirements and carbon emissions by as much as 10% compared to plain Portland cement while producing eco-concretes with comparable performance [5,42]. Thus, the use of composite Portland cements, such as CEM II, represent one component of the cement industry's environmental footprint reduction strategy [7]. As such, sub-type CEM II/A cement is currently the most consumed in Europe [43].

Table 1 lists the bulk chemical compositions, physical properties and pozzolanicity of the binding materials, as well as the chemical requirements of FA for use in concrete defined by EN 450-1 standard. Chemical composition was obtained by X-ray fluorescence spectrometry, and loss on ignition was evaluated following European standard EN 196-2.

Considering the cement chemical composition, its constituents' content was determined as follows: mass percentage of gypsum = $1.6 \times \text{mass percentage of } \text{SO}_3 = 4.35\%$ and mass percentage of filler = $2 \times \text{loss on ignition (500–950 } ^\circ\text{C)} = 12.50\%$. Thus, the mass percentage of clinker is 83.15%.

Results show that ECat meets the normative chemical requirements of FA for use as an addition in concrete. The quality of the ECat regarding loss on ignition is higher than that of FA, as ECat complies with category A, and FA with category B.

Density was determined by helium pycnometry. Specific surface area was determined by nitrogen adsorption-desorption isotherm at 77 K.

Particle size distribution was obtained by laser diffraction. Figure 1a shows the cumulative particle size distributions of binding materials. The fineness of FA particles is similar to those of CEM II particles both regarding the median (d_{50}) and particle size distribution (although the mean of FA particles is higher than that of CEM II); whereas ECat particles are significantly coarser and have a narrower particle size distribution than those of CEM II and FA. Thus, besides the pozzolanic effect, FA particles may promote a filler effect associated with their ability to deposit in the intergranular voids between cement particles, which should contribute to a denser cement mortar matrix. The filler effect due to ECat is not expected to be significant [44].

FA and ECat pozzolanicity was evaluated, both directly using the modified Chapelle test (described in French standard NF P 18-513), and indirectly using the activity index (AI) according to European standard EN 450-1. AI is the ratio (in percent) between the compressive strength of a mortar sample, prepared with 75% (by mass) cement CEM I 42.5R and 25% pozzolan (FA or ECat) by the compressive strength of a mortar sample prepared with 100% cement, at the same curing age.

The results show that both FA and ECat are pozzolanic materials, since they react with Ca(OH)_2 . Direct determination of Ca(OH)_2 by Chapelle's test show that ECat presents a high pozzolanic reactivity since it consumes 1540 mg/g (Table 1) while, typically, pozzolans consumes lower than 1000 mg of lime per g of tested material [45]. This result is in accordance with the ECat's very high specific surface area of 150070 m^2/kg (Table 1). From this test result, FA also presents a significant pozzolanic reactivity—consuming 991 $\text{mg}_{\text{lime}}/\text{g}$ (Table 1)—although lower than that of ECat. According to the EN

450-1 standard, a material is pozzolanic if, at 28 days of curing age, $AI \geq 75\%$. Since AI values of FA and ECat are higher than 83%, this test method confirmed both additions of pozzolanicity. However, since the AI values are similar for both additions, the indirect test method to evaluate the pozzolan activity by computing AI do not reflect the higher ECat pozzolanicity shown in the Chappelle's test result. This result, i.e., the similarity between the AI values for both additions, might be attributed to a lack of $Ca(OH)_2$ available in the hydrated cement matrix, due to the significant cement replacement level with the pozzolanic materials (25%, by mass) in the blended binder mortar prepared to determine pozzolans' AI. This argument is reinforced by the fact that, in a previous study [34], in which pozzolanicity of ECat, at 28 days, was evaluated by preparing the blended cement mortar with a lower cement replacement level with ECat of 20% (by mass) (as prescribed by the American standard ASTM C311), the AI value obtained was 95%. Thus, it seems that the mortar with higher cement content that forms more cement hydration products, such as $Ca(OH)_2$, increases the extension of the ECat's pozzolanic reaction.

Table 1. Chemical composition, physical properties and pozzolanicity of binding materials as well chemical properties of fly ash (FA) for use in concrete defined by EN 450-1 standard.

	CEM II/A-L	Fly Ash	ECat	EN 450-1
Chemical Composition (% by Mass)				
SiO ₂	17.56	56.04	40.30	SiO ₂ + Al ₂ O ₃ + Fe ₂ O ₃ > 70
Al ₂ O ₃	4.80	23.05	54.45	
Fe ₂ O ₃	3.16	8.03	0.45	
CaO	61.78	3.73	0.06	
MgO	1.68	1.71	0.15	<10
SO ₃	2.72	0.25	0.00	<4
K ₂ O	0.86	1.63	0.02	<3
Na ₂ O	0.03	0.66	0.43	K ₂ O + Na ₂ O < 5
TiO ₂	0.25	1.13	0.72	
P ₂ O ₅	0.06	0.50	0.50	<5
MnO	0.05	0.06	0.00	
SrO	0.07	0.09	0.00	<5, class A; <7, class B
V ₂ O ₅	0.00	0.00	0.33	
NiO	0.00	0.00	0.42	
La ₂ O ₃	0.00	0.00	0.87	
LOI ¹ (110–250 °C)	0.11	-	-	<5, class A; <7, class B
LOI ¹ (250–500 °C)	0.16	-	-	
LOI ¹ (500–950 °C)	6.25	-	-	
LOI ¹	6.51	6.57	1.05	<5, class A; <7, class B
Total	99.53	99.43	99.75	
Physical Properties				
Density	3.11	2.38	2.69	
Surface area, SSA (m ² /kg)	1156	2020	150070	
Mean of particles size (μm)	18.95	29.50	91.65	
d ₅₀ ² (μm)	16.21	16.61	87.29	
d ₉₀ ² (μm)	40.59	73.90	138.11	
Pozzolamicity				
Modified Chapelle test result (mg of Ca(OH) ₂ per g of pozzolan)	-	991	1540	
Activity Index-AI (%), 28 days	-	83.4	83.6	

¹ LOI: Loss on ignition; ² d₅₀, d₉₀: 50% and 90% (v/v), respectively, of particles have diameters smaller than the presented value.

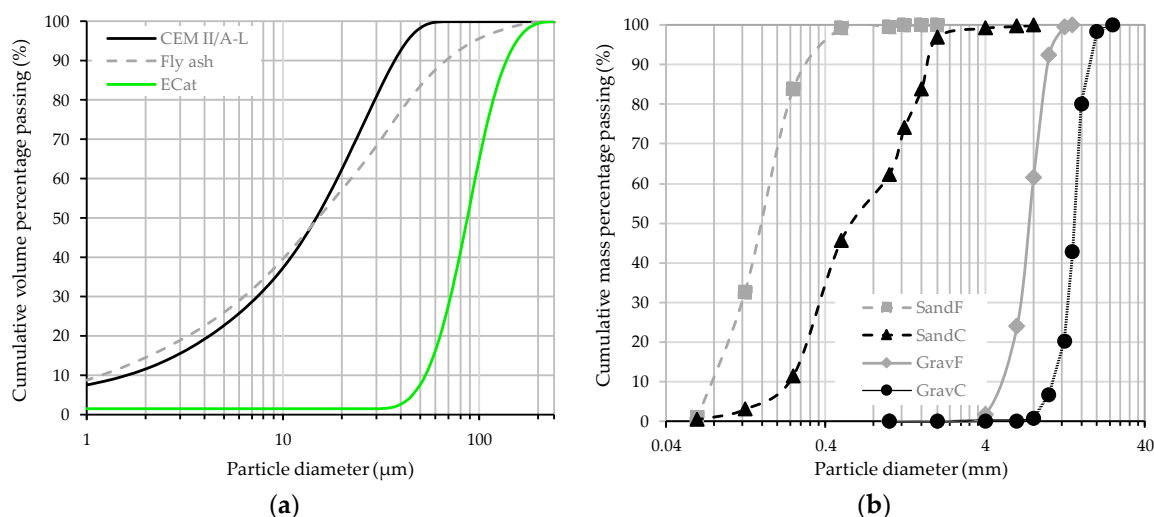


Figure 1. Cumulative particle size distributions of (a) binding materials and (b) aggregates.

Four different aggregates (according to European standard EN 12620) were used: two different natural siliceous sands, one coarser designated SandC, (density 2.63, fineness modulus of 5.23, water absorption of 0.77%) and one finer designated SandF (density 2.63, fineness modulus of 2.84, water absorption of 0.48%) as well as two crushed limestone gravels, one coarser designated GravC (density 2.69, fineness modulus of 8.51, shape index of 19.30, water absorption of 1.1%) and one finer designated GravF (density 2.72, fineness modulus of 5.21, shape index of 19.50, water absorption of 1.0%). Figure 1b shows the cumulative particle size distributions of aggregates determined following the EN 933-2 standard.

Two concrete admixtures were used: the third-generation high-range water reducer superplasticizer (Sp) BASF MasterEase 3530 and the plasticizer (P) MasterPozzolith 7002, both complying with European standard EN 934-2. The Sp consists of modified polycarboxylates and P consists of lignosulfonate and both are supplied in liquid form with a density of 1.07 and 1.11, respectively. Tap water was used, in accordance with European standard EN 1008.

The materials used in this study, except for the ECat, are the same of those used in the industrial ready-mixed concrete production at Betão Liz.

2.2. Concrete Mixture Design and Samples Preparation

Four concrete mixtures with binary and ternary blended binders comprising CEM II, FA and ECat, were investigated. The reference concrete has a binary blended binder containing 66.7% (by mass) of CEM II and 33.3% (by mass) of FA. This reference concrete mixture reproduces the formulation of a concrete, widely used in ready-mixed concrete plants of Betão Liz company, that complies with C25/30 XC2(P) C1 0.2 Dmax22 S4 class of concrete in accordance with the EN 206-1 standard. Since the investigation intended to be industrial application-oriented, the innovative concretes mixtures were designed to assess if the same clinker factor reduction can be achieved. As such, the other three concretes tested incorporate ECat in their binders as a partial, or total, surrogate of the FA present in the reference concrete.

The acronyms adopted in this study for the concrete mixtures identification refer the percentage (by mass) of each addition present in the binder as follows: 33FA is the reference industrial concrete mixture, 16FA16ECat is the concrete which binder's phase contains 16.7% of FA and 16.7% of ECat and, 16ECat and 33ECat are, respectively, the concretes which binder's phases contain 16.7% and 33.3% of ECat. Table 2 presents the mixture proportions of concretes.

Table 2. Mixture proportions of the concretes (values in brackets corresponds to the mass percentage of each constituent in the binder).

Concretes Acronyms	Binder Phase (B)			SandF	SandC	GravF	GravC	SP	P	Water (w)	w _{added} /B	w _{eff} /B
	CEM II	FA	ECat									
	(Kg/m ³)											
33FA (Reference mix)	200 (66.7%)	100 (33.3%)	0	300	580	540	540	1.5	1.5	148	0.49	0.49
16FA16ECat	200 (66.7%)	50 (16.7%)	50 (16.7%)	300	560	540	540	1.5	1.5	165	0.55	0.50
16ECat	250 (83.3%)	0	50 (16.7%)	320	560	520	520	1.5	1.5	175	0.58	0.53
33ECat	200 (66.7%)	0	100 (33.3%)	320	560	520	520	1.5	1.5	188	0.63	0.53

w_{added}/B —water-to-binder mass ratio; w_{eff}/B —effective water-to-binder mass ratio.

The simultaneous use of cement type CEM II and a high content of additions in the concrete composition is aligned with the action plan developed by the ready-mixed concrete sector strategy to improve resource efficiency and reduce concrete embodied carbon, and thus, increasing its sustainability [46].

The small adjustments in the aggregates composition of the concretes with ECat incorporation (Table 2) were established based on preliminary mixture preparation, to ensure similar visual appearance of concretes in the fresh state and, thus, to preserve end-user acceptance. The water content was also experimentally calibrated to keep a constant slump value of 200 ± 10 mm in the range (160–210 mm) of the S4 concrete consistency class. As anticipated based on previous results [34,36,40] the water needed to achieve similar slump values tend to increase with the increase of ECat content due to its very high specific surface ($150070 \text{ m}^2/\text{kg}$, Table 1) with water affinity that promotes a significant water absorption of 29.7% (by mass). In fact, the water content increases 27.0% from 148 kg/m^3 in the 33FA reference concrete to 188 kg/m^3 in the 33ECat concrete which corresponds, respectively, to w_{added}/B ratios of 0.49 and 0.63. However, the determination of the effective water-to-binder mass ratio, w_{eff}/B , (Table 2), using Equation (1), reveals that the effective water available for binder hydration was kept mostly the same among the concretes, varying in a much narrower range within 0.49 and 0.53. Thus, the excess water added in concretes with ECat incorporation is absorbed by its particles, not remaining as free water.

$$\frac{w_{\text{eff}}}{B} = \frac{w_{\text{added}} - \text{water theoretically absorbed by ECat } (0.297 \times \text{ECat content})}{B} \quad (1)$$

where w_{added} is the added water, and ECat and B are the ECat and binder content in concrete expressed in kg/m^3 , respectively.

Concrete mixtures were prepared using a vertical axis mixer following the procedure presented in Table 3. Just after mixing, the following properties of fresh concretes were evaluated (following the standard test methods mentioned between parentheses): consistency by slump test (EN 12350-2), and bulk density (EN 12350-6).

Table 3. Concrete mixing procedure.

Task	Duration
wipe the inside of the mixing bowl with a damp cloth	-
introduce the dry aggregates (in descending order of particle size) with 5% of water and mix	1.0 min
resting	4.0 min
add cement + additions + 70% of water and mix	1.0 min
add remaining water + superplasticizer + plasticizer and mix	2.0 min
resting (and scrape material adhering to the mixing bowl)	2.0 min
final mix	2.0 min

For each concrete mixture, various samples were prepared for posterior testing in the hardened state. As such, molds were filled and compacted following the EN 12390-2 standard. Depending on the property to be evaluated, different molds' shape and size were adopted (Section 2.3) namely, cubic molds with 150 mm side for compressive strength and ultrasonic testing, and cylindrical molds ($\varnothing 100$ mm \times 200 mm) for chloride migration, electrical resistivity and water capillary absorption testing. The samples were unmolded after 24 h and stored in a chamber at 20 ± 2 °C and humidity greater than 95% until testing date. Three samples were tested for each test property and curing age.

2.3. Experimental Design and Test Methods on Hardened Concrete

2.3.1. Experimental Design

The use of complex concrete mixtures, namely incorporating recycled products, endorse a performance-based mixture design approach concerning the mechanical properties and the durability.

Mechanical properties evaluated were the compressive strength and the dynamic modulus of elasticity (E_d). This property was determined from ultrasonic pulse velocity (UPV) measurements because this method has proved to be useful, reliable and non-destructive both for computing E_d and to estimate concrete quality.

Concrete durability is largely related to the ingress of deleterious external agents that could lead to deterioration of concrete performance over time. As such, the durability depends on the microstructure of the material (pore size distribution, connectivity and tortuosity of pore system as well as chemistry) that determines the mechanisms of substances penetration in concrete. Typically, a single parameter is not sufficient to characterize the 'potential' durability of concrete, namely regarding corrosion, due to the physicochemical complexity of processes that take place as well as due to the different driving forces involved in the transport of substances such as, concentration gradient and total pressure gradient.

The key transport properties assessed were: (i) capillary water absorption that governs the liquid moisture movement by surface tension effects. This is one of the most important features of a building material because is considered the fastest transport mechanism and may occur in a dry or semi-dry state; (ii) chloride ions migration since chloride ions can trigger reinforcement corrosion which is a major issue for the durability of concrete structures; and (iii) electrical resistivity that indicates the ability to transport the electrical charges through the material. This property besides depending on pore structure is also influenced by the composition of the pore solution. Since corrosion is an electrochemical process, resistivity also correlates with reinforcement corrosion potential.

The 'potential' durability of a given concrete mixture is specified from its classification based on transport properties values experimentally obtained. The durability classes were defined based on threshold values of the transport properties referred to as durability indicators (see Sections 3.2.4 and 3.2.5).

2.3.2. Test Methods

The compressive strength test was performed at 7, 28 and 91 days following the procedure described in European standard EN 12390-3.

Ultrasonic pulse velocity (UPV) was evaluated at 1, 2, 3, 6, 7, 14, 28, 56 and 91 days. UPV was measured by direct transmission method (following the procedure described in EN 12504-4 standard) using a PROCEQ Tico test equipment with two 54 kHz transducers. UPV values were computed using Equation (2).

$$UPV = \frac{L}{t} \text{ (km/s)} \quad (2)$$

where, L is the ultrasonic pulse path length through the sample i.e., the distance between the two transducers and t is the pulse transit time provided by the test equipment.

The dynamic modulus of elasticity (E_d) of concretes was determined from the UPV values using the Equation (3) [47].

$$E_d = \text{UPV}^2 \cdot \rho' \cdot \frac{(1 + \nu)(1 - 2\nu)}{(1 - \nu)} \quad (\text{MPa}) \quad (3)$$

where E_d is the dynamic modulus of elasticity (MPa); UPV is the ultrasonic pulse velocity (km/s) obtained by Equation (2); ρ' is the density of hardened concrete (kg/m^3) computed by dividing the sample mass (experimentally assessed before the UPV test) to its volume (0.15^3 m^3); and ν is the dynamic Poisson's ratio, assumed 0.2 in this study since it is a typical value for normal concretes [48].

The resistance to capillary water absorption of concretes, at 28 and 91 days, was evaluated following the testing procedure described in the EN 13057 standard. In brief, the procedure consisted in preparing, for each concrete mixture, three replicates samples ($\varnothing 100 \times 100 \text{ mm}$) sliced from the cylindrical samples molded. After that, the measurements of water capillary absorption were carried out immersing 2 mm of the cut face of each dried sample into water. The mass of each sample was monitored after 12 min, 30 min, 1 h, 2 h, 4 h and 24 h from its first contact with water. The water uptake per unit area was calculated, for each time increment, from the mass of water absorbed (kg) divided by the cross-sectional area of the test face exposed to water (m^2). The capillary water sorption coefficient, S ($\text{kg}/\text{m}^2 \cdot \text{h}^{0.5}$), is obtained empirically from the slope of the plot of the water uptake per unit area (kg/m^2) against the square root of time of immersion ($\text{h}^{0.5}$).

The chloride migration coefficient of concretes at 28 and 91 days was evaluated from non-steady state migration experiments following the testing procedure described in NT BUILD 492 standard. In brief, the procedure consisted in preparing, for each concrete mixture, three replicates samples ($\varnothing 100 \times 50 \text{ mm}$) sliced from the cylindrical samples molded. The samples were vacuum soaked with a $\text{Ca}(\text{OH})_2$ saturated solution and, thereafter, an electrical potential is applied to force chloride ions to migrate (from a 10% NaCl catholyte solution) through the samples. Each sample was subsequently axially split into two pieces, and the freshly broken surfaces were sprayed with 0.1 M silver nitrate solution. The chloride migration depth was established as the depth of visible white silver chloride precipitated. The non-steady state chloride migration coefficients, D_{nssm} , were determined using Equation (4).

$$D_{\text{nssm}} = \frac{0.0239(273 + T)L}{(U - 2)t} \times \left(x_d - 0.0238 \sqrt{\frac{(273 + T)Lx_d}{U - 2}} \right) \times 10^{-12} \quad (\text{m}^2/\text{s}) \quad (4)$$

where U is the absolute value of the applied voltage (V); T is the average value of the initial and final temperatures in the 0.3 M NaOH anolyte solution (K); L is the measured values of specimen thickness (mm); x_d is the average value of the penetration depths (mm); and t is the test duration (h).

The electrical resistivity (ρ) of concretes was evaluated at 7, 9, 11, 14, 21, 28, 56 and 91 days using the two electrodes technique. Electrodes were composed of wet sponges in contact with stainless steel plates ($\varnothing 100 \text{ mm}$ and 2 mm thick) placed on the saturated flat faces of the samples prepared for the chloride migration experiments. The electrical current intensity was monitored by applying a force (to ensure a constant and uniform stress distribution over the entire sample face) and 60 V voltage. The electrical resistivity (ρ) was then computed using Ohm's Law (Equation (5)).

$$\rho = \frac{V}{I} \frac{A}{L} \quad (\Omega \cdot \text{m}) \quad (5)$$

where V is the applied voltage (Volts); I , current intensity (Ampere); and, A and L are, respectively, the cross-sectional area (m^2) and length (m) of the test sample through which current passes.

3. Test Results and Discussion

3.1. Fresh State

Table 4 shows the properties of concretes in the fresh state. As previously discussed (Section 2.2), the amount of water added to the concrete mixtures was adjusted to obtain a target slump value of 200 ± 10 mm. The difference between the highest value of density exhibited by the concrete 33FA and the lowest presented by 33ECat is only 2.9% and, thus, negligible. Even though, results show that incorporation of ECat in the binders tends to decrease the concretes densities in the fresh state.

Table 4. Properties of concretes in the fresh state.

Property/Concretes	33FA	16FA16ECat	16ECat	33ECat
Slump (mm)	200	200	200	190
Density (Kg/m ³)	2437	2415	2408	2366

3.2. Hardened State

3.2.1. Compressive Strength

Figure 2 shows the compressive strength development of the binary and ternary blended binder concretes under investigation. At 7 days of curing age, the binary blended binder concrete, 16ECat, exhibited the highest strength of 34.1 MPa, which is slightly higher than those exhibited by the reference industrial ready-mix concrete, 33FA, of 32.0 MPa and by the ternary blended binder concrete, 16FA16ECat, of 31.0 MPa. At this curing age, the binary blended binder concrete with more ECat content, 33ECat, showed the lowest strength of 24.2 MPa. In fact, this difference in the strength of 33ECat c.a. of 20% lower than that of the reference concrete remained up to 90 days. At 28 days, the concrete 16ECat still showed the highest strength of 49.4 MPa, as well as concretes 33FA and 16FA16ECat remained with lower strengths (of 44.2 and 43.3 MPa, respectively) and similar to each other. However, from this curing age, 16ECat concrete showed almost no strength gain, whereas all other concretes, mainly 33FA, showed a continuous gain in strength, reaching at 90 days the strength values of 55.4, 51.2 and 43.3 MPa for 33FA, 16FA16ECat and 33ECat, respectively.

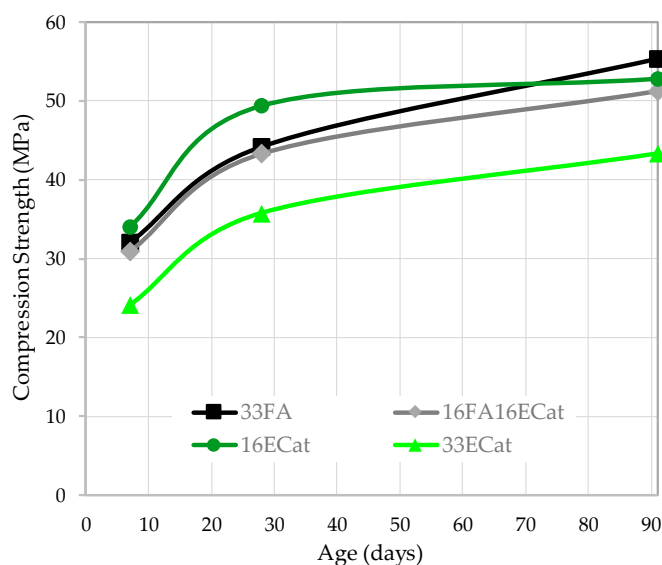


Figure 2. Compressive strength development of concretes over curing age.

Figure 2 also reveals that the total additions content in the binder does not determine the compressive strength development over time. In fact, although the three concretes 33FA, 16FA16ECat and 33ECat have 33% of additions incorporation, the 33ECat concrete presented lower compressive strength than those of concretes with the same content of FA and the same total content of additions of half of each, FA and ECat. These might be attributed to the differences in the additions properties. Namely, FA particles are finer than those of ECat and present a polydisperse size distribution, while ECat particles are nearly monodispersive (Figure 1a). Therefore, the filling ability of the FA particles (Section 2.1) also contributes to the higher strength exhibited by concretes with this addition incorporation [44].

ECat exhibited a higher pozzolanic reactivity, assessed by the Chappelle test, than FA (1540 and 991 mg/g, respectively) and similarly, pozzolanicity assessed through AI (83.6% and 83.4%, respectively, Table 1). This means that the pozzolanic effect of the ECat in the cement matrix might have been limited by the absence of free calcium hydroxide ($\text{Ca}(\text{OH})_2$), liberated by clinker hydration, since limestone Portland cement had been used in this study. In fact, the clinker content in the concretes binder's composition with CEM II/A, and 33% of additions is only 55.5%, by mass. This explanation seems to be reinforced by the faster and higher strength development of the 16ECat concrete (up to 28 days), which has the highest cement, and thus, clinker content in the binder (Table 2). The confirmation of this hypothesis requires further investigation of $\text{Ca}(\text{OH})_2$, e.g., using thermo-gravimetric analysis or X-ray diffraction techniques. However, this deficiency in $\text{Ca}(\text{OH})_2$ compromising ECat's pozzolanic activity has been verified elsewhere [49].

From a technological perspective, the concretes with ECat incorporation achieved the compressive strength values specified in the EN 206-1 standard for a concrete strength class C25/30.

3.2.2. Ultrasonic Pulse Velocity

Figure 3 presents the evolution of the UPV and dynamic modulus of elasticity (E_d) results of concretes over time. The UPV values increase over time reaching an asymptotic maximum velocity value beyond a given curing age, as expected [50]. The concretes under study approached the maximum value at 14 days of age. Moreover, the UPV values exhibited an inverse relationship with ECat content in the binders. As such, the asymptotic value of the 33FA zone is higher (ca. 3%) than those of 16FA16ECat and 16ECat, which are very similar between them, are in turn, are also ca. 3% higher than that of 33ECat concrete.

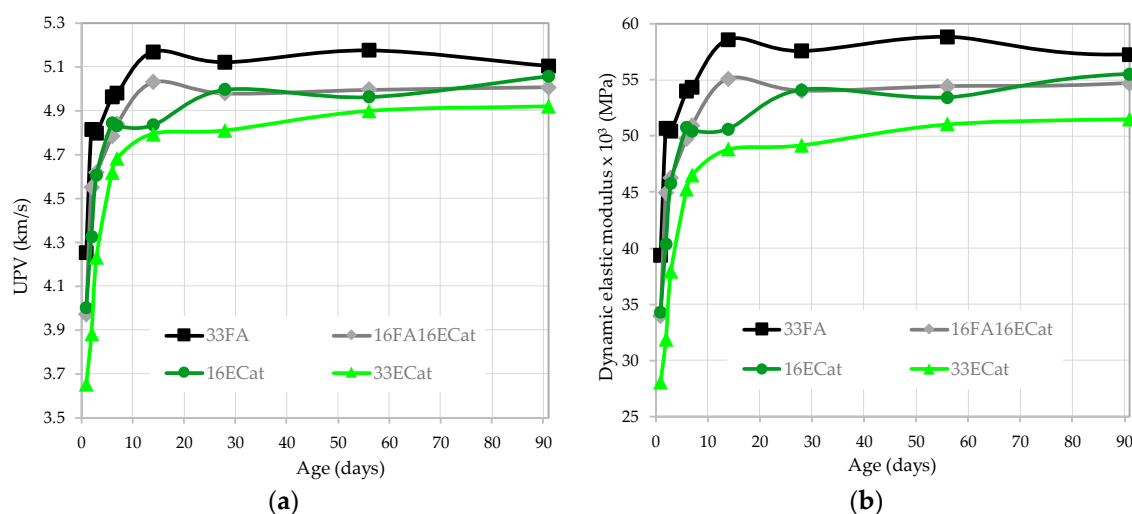


Figure 3. Evolution of (a) Ultrasonic Pulse Velocity (UPV) values and (b) elastic dynamic modulus (E_d) of concretes, over curing age.

However, considering a classification [51–53] to assess concrete quality based on UPV values presented in Table 5, all concretes fell within the range of ‘excellent’ beyond the sixth curing day. The ECat incorporation tended to slightly delay the achievement of the ‘excellent’ classification to 6 and 3 curing days for 33ECat and 16ECat, respectively, whereas the 33FA and 16FA16ECat reached this class from the 1st day.

Table 5. Concrete quality classification based on UPV values [51–53].

Concrete Quality	UPV (km/s)
Excellent	>4.5
Good	3.6–4.5
Questionable	3.0–3.6
Poor	2.1–3.0
Very Poor	<2.1

The concretes with ECat incorporation present lower E_d values than that of the binary blended binder with FA, 33FA (Figure 3b). The trend of the E_d plots against time is similar to those of the UPV. However, the relative difference among the values for the diverse concretes are higher, i.e., 33FA has E_d values, on average, 6.5% higher than those of 16FA16ECat and 16ECat, which are very similar between them and that have E_d values, after the third day, 7% on average higher than those of 33ECat.

Although there is no precise form of the relationship, there is a general agreement that the modulus of elasticity increases with an increase in the compressive strength of concrete. Thus, it would be expected that the elastic modulus of 16ECat would be the highest, at least during the first stages, since it is the concrete which exhibited the highest strength (Figure 2), but this was not verified (Figure 3b).

3.2.3. Capillary Water Absorption

Figure 4 plots the capillarity water uptake against the time of immersion in water after 28 and 90 days of curing age. Table 6 presents the corresponding capillary sorption coefficients, S , i.e., the slopes of the linear fit of capillary water uptake experimental results against the square root of the time as well as the fitting correlation coefficient (R^2).

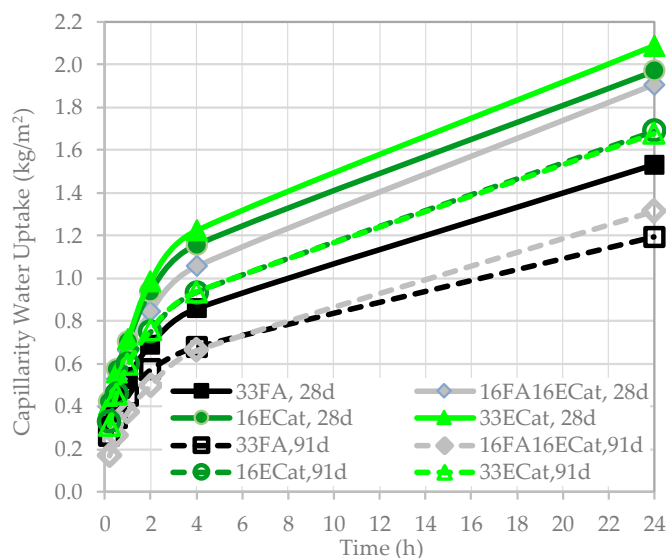


Figure 4. Capillarity water uptake of concretes against water immersion time at 28 and 90 days of curing age.

Table 6. Capillary water sorption coefficients, S , and the linear fitting correlation coefficient (R^2) after 28 and 90 curing days of concretes.

Concrete	28 Days		90 Days	
	S (kg/m ² ·h ^{0.5} or mm/h ^{0.5}) *	R^2	S (kg/m ² ·h ^{0.5} or mm/h ^{0.5}) *	R^2
33FA	0.26	0.99	0.20	0.98
16FA16ECat	0.33	0.99	0.25	0.99
16ECat	0.34	0.98	0.30	0.98
33ECat	0.37	0.97	0.30	0.99

* Since water density is 1000 kg/m³, dividing S expressed kg/m²·h^{0.5} by water density value, gives the same value of S expressed in mm/h^{0.5}.

Figure 4 and Table 6 show that for all concretes investigated both water uptake and sorption coefficients decrease from 28 to 90 days of age, as expected, in a range from 12.4% for 16ECat to 24.1% for 16FA16ECat. Moreover, concretes with ECat incorporation have higher S values of 26.9% for 16FA16ECat, 30.8% for 16ECat and 42.3% for 33ECat at 28 days of age and 25.0% for 16FA16ECat and 50.0% for both 16ECat and 33ECat at 90 days of age. Thus, an overall analysis of these results reveals that typically ECat, in these concretes composition, promotes an increase in water permeability.

Typically, the pozzolanic reaction product formation promotes a decrease in the volume of capillary pores and their interconnectivity and, thus, an increase in the water absorption resistance [54]. This effect has been found in studies using ECat generated in the same [37,38], and other refineries [55] as cement surrogate up to 20%.

However, the findings of the current investigation (Table 6) show that, in general, the increase of the ECat in the binder leads to an increase in the capillary water absorption of concrete, which has also been previously seen elsewhere for high levels ECat incorporation in the binder above 20% [35,56]. Therefore, this effect emphasizes the assumption mentioned above, that the occurrence of the pozzolanic reaction of ECat, when it is present in the binder beyond a particular content, might be limited by the absence Ca(OH)₂ due to the small amount of clinker.

The criteria, available in the literature [57], to assess the concrete quality based on water absorption, refers that for $S < 5$ mm/h^{0.5} concretes are of very good quality. Since, S values obtained for all investigated concretes (Table 6) are markedly smaller than that threshold S value all concretes possess a high potential of durability regarding this property.

3.2.4. Chloride Migration

Figure 5 presents the non-steady state chloride migration coefficients, D_{nssm} , of concretes at 28 and 91 days of curing. The figure also shows (by means of horizontal lines) the range of D_{nssm} ($\times 10^{-12}$ m²/s) values that determine the concretes classification of 'potential' durability against chloride-induced corrosion [58]. The classes are the following: Very Low (VL) for $D_{nssm} > 50$, Low (L) for $D_{nssm} = 10$ to 50, Medium (M) for $D_{nssm} = 5$ to 10, High (H) for $D_{nssm} = 1$ to 5 and Very High (VH) for $D_{nssm} < 1$.

The results show (Figure 5) a marked decrease in D_{nssm} values for the higher curing ages in a range of 94.4% for 16ECat to 98.3% for 33FA. This increasing resistance against chloride ingress over time was anticipated due to the continued binder hydration that leads to the refinement of capillary pore structure. For the investigated concretes, the chloride migration was more affected by the blended cement pastes densification over time than the water absorption by capillarity (Table 6).

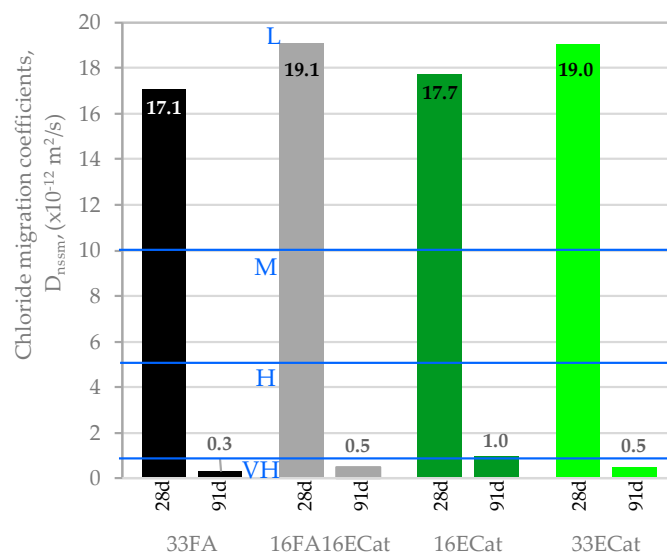


Figure 5. Non-steady state chloride migration coefficients, D_{nssm} , of concretes at 28 and 90 days of curing age as well as their potential durability classification against external chloride attack (VH, very high; H, high; M, medium; L, low).

At 28 days of curing age, the concretes with 33% of additions incorporation containing ECat, 16FA16ECat and 33ECat, exhibit an increase of around 11.5% in the D_{nssm} values in relation to the reference concrete (33FA), whereas for concrete with 16% of ECat incorporation the D_{nssm} value is similar with that of 33FA. At 91 days, D_{nssm} values of concretes with ECat incorporation increase regarding that of 33FA, being the D_{nssm} value of 16ECat the highest. However, considering the heterogeneity of the concretes, and that the standard deviation (SD) of the migration coefficients, D_{nssm} , is about $0.98 \times 10^{-12} \text{ m}^2/\text{s}$ [59], too much relevance should not be attributed to the differences in D_{nssm} values obtained for the different concretes at 91 days, since they are within the SD limits. As such, it can be reasoned that at this curing age, the chloride ingress resistance is very high and the difference among the tested concretes is negligible.

Previous studies have revealed that the incorporation of up to 30% of ECat in the binder promotes an increase in the chloride penetration resistance in relation to that of plain cement [37,38,60] and also that ternary blended binders with 30% of FA and ECat hinders the chloride ingress in relation to binary blended binders with only FA [41]. The increment in resistance against chloride ions migration was attributed to additional densification of the pozzolan blended cement pastes, namely with ECat, associated with its exceptional pozzolanic reactivity forming reaction products, refine the capillary pore sizes. Nevertheless, similar results were not found in the current investigation. In line with the above-mentioned arguments, one consideration is that the use of CEM II type of cement (instead of CEM I used in the studies reported in the literature) lowered the clinker content to the point that might have compromised the availability of the required $\text{Ca}(\text{OH})_2$ to ensure the ECat pozzolanic reaction occurrence.

All investigated concretes, at 90 days of age, had values of $D_{nssm} \leq 1 \times 10^{-12} \text{ m}^2/\text{s}$ (Figure 5). As such, all concretes' durability class is VH meaning that from the technological viewpoint ECat shall not increase the risk of corrosion of the reinforcement of concretes under external chloride attack.

3.2.5. Electrical Resistivity

Figure 6 presents the evolution of electrical resistivity (ρ) results of concretes over time. The figure also points out (by means of horizontal lines) the range of values proposed elsewhere [58] to classify the 'potential' durability of concretes concerning reinforcement corrosion based on ρ values. These classes are: very low (VL) potential durability for $\rho < 50 \Omega \text{ m}$, low (L) for $50 < \rho < 100 \Omega \text{ m}$, medium (M) for $100 < \rho < 250 \Omega \text{ m}$, high (H) for $250 < \rho < 1000 \Omega \text{ m}$ and very high (VH) for $\rho > 1000 \Omega \text{ m}$.

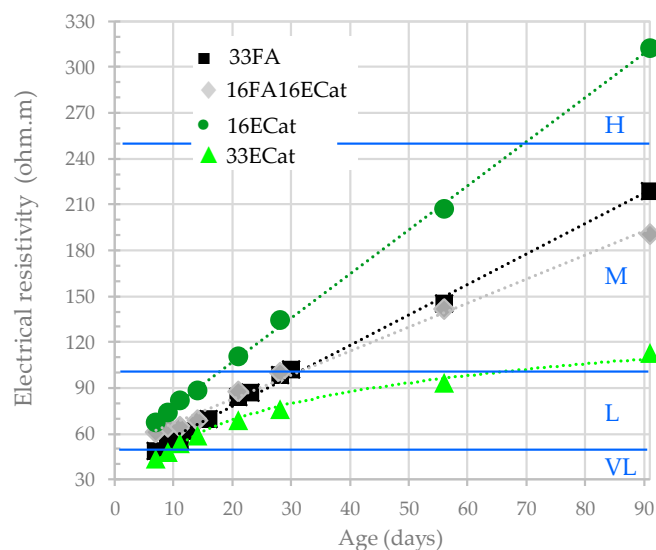


Figure 6. Evolution of the experimental results of electrical resistivity of concretes over curing age as well as their potential durability classification concerning reinforcement corrosion (VL, very low; L, low; M, medium; H, high).

Since the electrical resistivity is the material property that evaluates its resistance against the flow of the electrical current (which is mainly carried via the ions present in the liquid phase), it is mostly dependent on pore network connectivity and ions concentration [61]. Therefore, as expected, the results show (Figure 6) that electrical resistivity increases with the binder hydration progress. In fact, 33FA, 16FA16ECat and 16ECat exhibit a significant linear increase of ρ results with time up to 91 days of curing, respectively of 346.4% (from 49.0 Ω m), 210.6% (from 61.4 Ω m), and 363.0% (from 67.45 Ω m) whereas 33ECat display a logarithmic behavior increasing 158.9% (from 43.4 to 112.8 Ω m).

The densification of concrete microstructure that corresponds to a more refined capillary pore system and thus, higher electrical resistivity typically also promotes the increasing of compressive strength, UPV, modulus of elasticity as well as of the resistance against capillary water absorption and chloride migration. Unambiguous relationships among these properties are not yet established for all concretes, because they are all affected in different ways by several factors that are also interdependent including, the raw materials properties, concretes preparation mode, cure conditions and test method adopted to evaluate properties of concretes [62]. However, the qualitative analysis of the results obtained in the current study shows that, in general, the ρ results obtained agree with those of the other properties. In fact, concretes with highest and lowest ρ values respectively, 16ECat and 33ECat also present the same relative position of compressive strength, UPV and modulus elasticity (Figures 2 and 3 respectively) and the reverse relative position in relation to capillary water uptake at 28 days (Figure 4). Likewise, the 16FA and 16FA16ECat that show similar ρ values present similar behavior in relation to compressive strength (Figure 2) and resistance against capillary water uptake (Figure 4) and comparable values of the other studied properties. However, the high increase in the resistivity values over time (Figure 6), mainly for 16ECat concrete, is not comparable with the level of increment in the compressive strength, which is much smaller. A possible explanation is that the pore refinement promoted by the pozzolans, namely the ECat to the cement matrix over time led to a more significant improvement of the durability properties than on the mechanical strength.

The presence of pozzolanic additions promote both changes in the concretes microstructure [54] and in the ionic composition of pores solution [63]. Thus, ρ values are also affected by the specific addition used. In fact, ρ results obtained for the investigated concretes lie in the same range of those reported elsewhere [45] for self-compacting mortars also incorporating ECat in their composition although the other mixtures constituents were not the same.

In view of their technological application and adopting the above mentioned classes of ‘potential’ durability of concretes regarding the reinforced corrosion estimated through the ρ values (pointed out in Figure 6) both concretes, 16FA16ECat and 16ECat, represent good alternatives in relation to the ready-mix industrial concrete used as reference, 33FA. In fact, both concretes with 33% of additions incorporation in the binder (33FA and 16FA16ECat) have, from 28 days until 90 days of age, the same medium-class of ‘potential’ durability, whereas 16ECat, although being slightly less eco-friendly, reaches the high-class of ‘potential’ durability before the 90 days of age.

4. Conclusions

This study intended to evaluate the feasibility of producing industrial ready-mixed eco-concretes incorporating ECat, a waste generated in the oil refinery industry. To pursue this objective, a widely industrially produced binary blended concrete with 33% FA, 33FA, was used as reference. ECat partially (16FA16ECat), or entirely (16ECat and 33ECat), surrogated FA in the innovative eco-concretes studied. The main conclusions of this investigation can be summarized as follows:

- The compressive strength development of 16FA16ECat concrete is similar to that of the reference concrete, 33FA. The 16ECat exhibits a strength gain higher than that of the 33FA up to 28 days whereas the compressive strength of the 33ECat is ca. 20% lower than that of 33FA up to 90 days of age. Anyhow, all concretes meet the target requirements of normative strength class C25/30
- Concretes with ECat incorporation present both lower UPV and dynamic elastic modulus values than those of 33FA concrete. Moreover, UPV and E_d values exhibit an inverse relationship with ECat content in the binders
- The classification scale to assess the concretes quality based on the UPV values reveals that all concretes are of ‘excellent’ quality
- The capillary water absorption, and the sorptivity, of ECat containing concretes are higher than those of the 33FA concrete. However, this increment shall not affect their technological application since, considering the criteria of potential durability of concretes based on S values, all investigated concretes are of ‘very good’ quality
- The non-steady state chloride migration coefficients, D_{nssm} , of all concretes markedly decrease from 28 to 91 days of age, and at this age, all have $D_{nssm} \leq 1 \times 10^{-12} \text{ m}^2/\text{s}$. As such, regarding the durability indicators established for this property, all concretes investigated, at 91 days, lie in the class interval of ‘very high’ resistance to chloride-induced corrosion
- Ternary 16FA16ECat concrete presents an electrical resistivity evolution similar to that of 33FA, 16ECat exhibits higher values and 33ECat lower than those of 33FA concrete. Once more these differences shall have no negative impact regarding their industrial application since, at 91 days, the 33ECat and 16FA16ECat concretes lie in the same class of durability (based on ρ values) than the 33FA, which is ‘medium’ and 16ECat belongs to the ‘high’ class.

In summary, ECat can be recycled in the production of ready-mixed concrete products, namely in the manufacture of 16FA16ECat and 16ECat concretes, with similar, or superior, technological performance, including durability when compared with that of current commercialisation. Both of these concretes contain 16.7% of ECat in binder’s phase and, respectively, 33.3% and 16.7% of total waste (ECat and FA) incorporation. Since concretes were prepared with limestone Portland cement type CEM II/A-L, the clinker content is 55.5% to 69.3%, respectively, for 16FA16ECat and 16ECat. Thus, these concretes also present sustainable qualities, including low carbon footprint and resource efficiency. Moreover, the results showed that the manufacture of ready-mixed ECat-incorporating concretes with the same clinker factor reduction (of 33%) of the current industrial production is feasible.

Likewise, ECat incorporation in concretes also provides environmental benefits to oil refinery industry due to landfilling reduction as well as economic advantages by adding value to a waste.

Further investigations will be carried out to optimize the composition of concretes with ECat incorporation that lead to the best performance targeting different engineer properties and, thus,

different applications. Taking in consideration the results presented in the current study, it is anticipated that the waste content in the concretes lie within the assessed range i.e., from 16.7% to 33% and that for most applications, the optimized ECat content shall be close to 16.7%.

Turning ECat into a steady supply for concrete manufacture industry fit in seamlessly with the scheme of the circular economy making a relevant contribution for a more dynamic and sustainable society.

Author Contributions: C.C. and J.C.M. conceived the research plan, supervised the experiments and analyzed the data; C.C. wrote the paper; J.C.M. revised the manuscript.

Funding: This research was financially supported by R&D Project with ref. IPL/2016/ECO-ZemLiz_ISEL funded by Instituto Politécnico de Lisboa.

Acknowledgments: This project builds upon research developed in ECO-Zement R&D+i project which was awarded with the Jerónimo Martins/Green Project Awards 2017. Acknowledgements are also due to Sines Refinery/Galp Energia for supplying ECat and to CIMPOR TEC, namely João Pereira, for the collaboration in the binding materials characterization. The assistance of Mário Costa for participating in the concrete testing is also gratefully acknowledged.

Conflicts of Interest: The authors declare no conflict of interest.

Abbreviations

AI	Activity index according to with European standard EN 450-1
B	Binder
D_{nssm}	Non-steady state chloride migration coefficient (m^2/s)
ECat	Spent equilibrium catalyst generated in oil-refinery
E_d	Dynamic modulus of elasticity (MPa)
FA	Fly-ashes
FCC	Fluid cracking catalytic
S	Capillary water sorption coefficient ($kg/m^2 \cdot h^{0.5}$)
UPV	Ultrasonic pulse velocity (Km/s)
w_{added}/B	Added water-to-binder mass ratio
w_{eff}/B	Effective water-to-binder mass ratio
ρ	Electrical resistivity

References

1. Meyer, C. The greening of the concrete industry. *Cem. Concr. Compos.* **2009**, *31*, 601–605. [CrossRef]
2. CEMBUREAU Key Facts and Figures. Available online: <https://cembureau.eu/cement-101/key-facts-figures/> (accessed on 16 July 2018).
3. The Concrete Initiative. Cement and Concrete Industry: Multiplier Effect on the Economy and Their Contribution to a Low Carbon Economy. 2015. Available online: <https://www.theconcreteinitiative.eu/newsroom/publications/143-cement-and-concrete-industry-multiplier-effect-on-the-economy-and-their-contribution-to-a-low-carbon-economy> (accessed on 3 July 2018).
4. Worrell, E.; Price, L.; Martin, N.; Hendriks, C.; Meida, L.O. Carbon Dioxide Emission from the Global Cement Industry. *Annu. Rev. Energy Environ.* **2001**, *26*, 303–329. [CrossRef]
5. Ishak, S.A.; Hashim, H. Low carbon measures for cement plant—A review. *J. Clean. Prod.* **2015**, *103*, 260–274. [CrossRef]
6. Feiz, R.; Ammenberg, J.; Baas, L.; Eklund, M.; Helgstrand, A.; Marshall, R. Improving the CO₂ performance of cement, part I: Utilizing life-cycle assessment and key performance indicators to assess development within the cement industry. *J. Clean. Prod.* **2015**, *98*, 272–281. [CrossRef]
7. WBCSD; IEA; Cement Technology Roadmap 2009. Carbon Emissions Reductions up to 2050. Available online: <https://www.iea.org/publications/freepublications/publication/Cement.pdf> (accessed on 3 July 2018).
8. CEMBUREAU Cement, Concrete & the Circular Economy. Available online: https://cembureau.eu/media/1229/9062_cembureau_cementconcretecirculareconomy_coprocessing_2016-09-01-04.pdf (accessed on 2 July 2018).
9. Liew, K.M.; Sojobi, A.O.; Zhang, L.W. Green concrete: Prospects and challenges. *Constr. Build. Mater.* **2017**, *156*, 1063–1095. [CrossRef]

10. Vishwakarma, V.; Ramachandran, D. Green Concrete mix using solid waste and nanoparticles as alternatives—A review. *Constr. Build. Mater.* **2018**, *162*, 96–103. [CrossRef]
11. Van Buren, N.; de Vries, M. Europe Goes Circular Outlining the Implementation of a Circular Economy in the European Area. 2017. Available online: https://www.rli.nl/sites/default/files/rli_eu_goes_circular_-_eeac_working_group_on_circular_economy_def_1.pdf (accessed on 3 July 2018).
12. EU. The EU Framework Programme for Research & Innovation HORIZON 2020. Available online: http://ec.europa.eu/programmes/horizon2020/sites/horizon2020/files/H2020_inBrief_EN_FinalBAT.pdf (accessed on 3 July 2018).
13. Aprianti, S.E. A huge number of artificial waste material can be supplementary cementitious material (SCM) for concrete production—A review part II. *J. Clean. Prod.* **2017**, *142*, 4178–4194. [CrossRef]
14. Shafigh, P.; Mahmud, H.B.; Jumaat, M.Z.; Zargar, M. Agricultural wastes as aggregate in concrete mixtures—A review. *Constr. Build. Mater.* **2014**, *53*, 110–117. [CrossRef]
15. Paris, J.M.; Roessler, J.G.; Ferraro, C.C.; Deford, H.D.; Townsend, T.G. A review of waste products utilized as supplements to Portland cement in concrete. *J. Clean. Prod.* **2016**, *121*, 1–18. [CrossRef]
16. Juenger, M.C.G.; Siddique, R. Recent advances in understanding the role of supplementary cementitious materials in concrete. *Cem. Concr. Res.* **2015**, *78*, 71–80. [CrossRef]
17. Costa, C. Hydraulic Binders. In *Materials for Construction and Civil Engineering: Science, Processing, and Design*; Gonçalves, M., Margarido, F., Eds.; Springer: Cham, Switzerland, 2015; pp. 1–52. [CrossRef]
18. Golewski, G.L. Green concrete composite incorporating fly ash with high strength and fracture toughness. *J. Clean. Prod.* **2018**, *172*, 218–226. [CrossRef]
19. Project COIN. *Fly Ash in Concrete. A Literature Study of the Advantages and Disadvantages*; SINTEF: Trondheim, Norway, 2009.
20. Ulubeyli, G.; Artir, R. Sustainability for Blast Furnace Slag: Use of Some Construction Wastes. *Procedia Soc. Behav. Sci.* **2015**, *195*, 2191–2198. [CrossRef]
21. Speight, J. *The Chemistry and Technology of Petroleum*, 4th ed.; Taylor & Francis Group, LLC, CRC Press: New York, NY, USA, 2006.
22. Ferella, F.; Innocenzi, V.; Maggiore, F. Oil refining spent catalysts: A review of possible recycling technologies. *Resour. Conserv. Recycl.* **2016**, *108*, 10–20. [CrossRef]
23. ECCPA. FCC Equilibrium Catalyst (Including FCC Catalyst Fines) Finds Safe Reuse/Rework Outlets in Europe. 2006. Available online: http://www.cefic.org/Documents/Other/Ecat_outlets_Europe_04Jan2006%20final%20Dec06.pdf (accessed on 3 July 2018).
24. Sines Refinery, Petroleos de Portugal PETROGAL, SA; Personal communication provided by Maria Santos; Environmental Manager at Petrogal, GalpEnergia: Sines, Portugal, 2017.
25. Sadeghbeigi, R. *Fluid Catalytic Cracking Handbook. An Expert Guide to the Practical Operation, Design, and Optimization of FCC Units*, 3rd ed.; Elsevier Inc.: Oxford, UK, 2012; ISBN 9780123869654.
26. Payá, J.; Monzó, J.; Borrachero, M.V. Physical, chemical and mechanical properties of fluid catalytic cracking catalyst residue (FC3R) blended cements. *Cem. Concr. Res.* **2001**, *31*, 57–61. [CrossRef]
27. Antiohos, S.K.; Chouliara, E.; Tsimas, S. Re-use of spent catalyst from oil-cracking refineries as supplementary cementing material. *China Part.* **2006**, *4*, 73–76. [CrossRef]
28. Paya, J.; Monzo, J.M.; Borrachero, M.V.; Velazquez, S. Pozzolan reaction rate of fluid catalytic cracking catalyst residue (FC3R) in cement pastes. *Adv. Cem. Res.* **2013**, *25*, 112–118. [CrossRef]
29. Wilińska, I.; Pacewska, B. Calorimetric and thermal analysis studies on the influence of waste aluminosilicate catalyst on the hydration of fly ash-cement paste. *J. Therm. Anal. Calorim.* **2014**, *116*, 689–697.
30. Silva, F.G.S.; Fiuza Junior, R.A.; da Silva, J.S.; de Brito, C.M.S.R.; Andrade, H.M.C.; Gonçalves, J.P. Consumption of calcium hydroxide and formation of C–S–H in cement pastes. *J. Therm. Anal. Calorim.* **2014**, *116*, 287–293. [CrossRef]
31. Lin, K.-L.; Wu, H.-H.; Chao, S.-J.; Cheng, A.; Hwang, C.-L. Characteristics of waste catalyst reused as latent hydraulic materials. *Environ. Prog. Sustain. Energy* **2013**, *32*, 94–98. [CrossRef]
32. Costa, C.; Ferreira, C.; Ribeiro, M.; Fernandes, A. Alkali-Activated Binders Produced from Petrochemical Fluid Catalytic Cracking Catalyst Waste. *Int. J.* **2014**, *3*, 114–122.
33. Tseng, Y.S.; Huang, C.L.; Hsu, K.C. The pozzolanic activity of a calcined waste FCC catalyst and its effect on the compressive strength of cementitious materials. *Cem. Concr. Res.* **2005**, *35*, 782–787. [CrossRef]

34. Costa, C.; Marques, P. Low-carbon cement with waste oil-cracking catalyst incorporation. In Proceedings of the IEEE Cement Industry Technical Conference, San Antonio, TX, USA, 14–17 May 2012. [CrossRef]
35. Torres Castellanos, N.; Torres Agredo, J.; Mejía de Gutiérrez, R.; Castellanos, N.; Agredo, J.; de Gutiérrez, R. Evaluation of the Permeation Properties of Concrete Added with a Petrochemical Industry Waste. *Calcined Clays Sustain. Concr. Bookser.* **2015**, *37*, 23–29. [CrossRef]
36. Payá, J.; Monzó, J.; Borrachero, M.V.; Velázquez, S. Cement equivalence factor evaluations for fluid catalytic cracking catalyst residue. *Cem. Concr. Compos.* **2013**, *39*, 12–17. [CrossRef]
37. Costa, C.; Ribeiro, M.S.; Brito, N. Effect of Waste Oil-Cracking Catalyst Incorporation on Durability of Mortars. *Mater. Sci. Appl.* **2014**, *5*, 905–914. [CrossRef]
38. Neves, R.; Vicente, C.; Castela, A.; Montemor, M.F. Durability performance of concrete incorporating spent fluid cracking catalyst. *Cem. Concr. Compos.* **2015**, *55*, 308–314. [CrossRef]
39. Castellanos, N.T.; Agredo, J.T. Using spent fluid catalytic cracking (FCC) catalyst as pozzolanic addition—A review. *Ing. Investig.* **2010**, *30*, 35–42.
40. Velázquez, S.; Monzó, J.; Borrachero, M.V.; Soriano, L.; Payá, J. Evaluation of the pozzolanic activity of spent FCC catalyst/fly ash mixtures in Portland cement pastes. *Thermochim. Acta* **2016**, *632*, 29–36. [CrossRef]
41. Zornoza, E.; Payá, J.; Garcés, P. Chloride-induced corrosion of steel embedded in mortars containing fly ash and spent cracking catalyst. *Corros. Sci.* **2008**, *50*, 1567–1575. [CrossRef]
42. Imbabi, M.S.; Carrigan, C.; McKenna, S. Trends and developments in green cement and concrete technology. *Int. J. Sustain. Built Environ.* **2012**, *1*, 194–216. [CrossRef]
43. CEMBUREAU. Cements for a Low-Carbon Europe—A Review of the Diverse Solutions Applied by the European Cement Industry through Clinker Substitution to Reducing the Carbon Footprint of Cement and Concrete in Europe. Available online: https://cembureau.eu/media/1501/cembureau_cementslowcarboneyurope.pdf (accessed on 3 July 2018).
44. Cyr, M.; Lawrence, P.; Ringot, E. Efficiency of mineral admixtures in mortars: Quantification of the physical and chemical effects of fine admixtures in relation with compressive strength. *Cem. Concr. Res.* **2006**, *36*, 264–277. [CrossRef]
45. Nunes, S.; Costa, C. Numerical optimization of self-compacting mortar mixture containing spent equilibrium catalyst from oil refinery. *J. Clean. Prod.* **2017**, *158*, 109–121. [CrossRef]
46. British Ready-Mixed Concrete Association. Ready-Mixed Concrete Resource Efficiency Action Plan British Ready-Mixed Concrete Association: London, UK. 2014. Available online: https://www.brmca.org.uk/documents/Ready_Mixed_Concrete_REAP_028_WRAP_BRE_BRMCA_Feb_14.pdf (accessed on 3 July 2018).
47. ASTM C597-16, Standard Test Method for Pulse Velocity Through Concrete. 2016. Available online: <https://shop.bsigroup.com/ProductDetail/?pid=000000000030344342> (accessed on 1 April 2016).
48. Neville, A.M. *Properties of Concrete*, 5th ed.; Pearson: London, UK, 2011; ISBN 0273755803.
49. Payá, J.; Monzó, J.; Borrachero, M.; Velázquez, S. Evaluation of the pozzolanic activity of fluid catalytic cracking catalyst residue (FC3R). Thermogravimetric analysis studies on FC3R-Portland cement pastes. *Cem. Concr. Res.* **2003**, *33*, 603–609. [CrossRef]
50. De Belie, N.; Grosse, C.; Baert, G. Ultrasonic transmission to monitor setting and hardening of fly ash concrete. *ACI Mater. J.* **2008**, *105*, 221–226. [CrossRef]
51. Leslie, J.R.; Cheeseman, W.J. An ultrasonic method for studying deterioration and cracking in concrete structures. *ACI Mater.* **1949**, *46*, 17–36.
52. Feldman, R.F. Non-Destructive Testing of Concrete, CBD-187. 1977. Available online: http://web.mit.edu/parmstr/Public/NRCAN/CanBldgDigests/cbd187_e.html (accessed on 1 May 2018).
53. Saint-Pierre, F.; Philibert, A.; Giroux, B.; Rivard, P. Concrete Quality Designation based on Ultrasonic Pulse Velocity. *Constr. Build. Mater.* **2016**, *125*, 1022–1027. [CrossRef]
54. Hossain, M.M.; Karim, M.R.; Hasan, M.; Hossain, M.K.; Zain, M.F.M. Durability of mortar and concrete made up of pozzolans as a partial replacement of cement: A review. *Constr. Build. Mater.* **2016**, *116*, 128–140. [CrossRef]
55. Pacewska, B.; Bukowska, M.; Wilińska, I.; Swat, M. Modification of the properties of concrete by a new pozzolan—A waste catalyst from the catalytic process in a fluidized bed. *Cem. Concr. Res.* **2002**, *32*, 145–152. [CrossRef]

56. Torres Castellanos, N.; Izquierdo García, S.; Torres Agredo, J.; Mejía de Gutiérrez, R. Resistance of blended concrete containing an industrial petrochemical residue to chloride ion penetration and carbonation. *Ing. Investig.* **2014**, *34*, 11–16. [[CrossRef](#)]
57. Bjegović, D.; Serdar, M.; Oslaković, I.S.; Jacobs, F.; Beushausen, H.; Andrade, C.; Monteiro, A.V.; Paulini, P.; Nanukuttan, S. Test methods for concrete durability indicators. *RILEM State Art Rep.* **2016**, *18*, 51–105. [[CrossRef](#)]
58. Baroghel-Bouny, V.; Kinomura, K.; Thiery, M.; Moscardelli, S. Easy assessment of durability indicators for service life prediction or quality control of concretes with high volumes of supplementary cementitious materials. *Cem. Concr. Compos.* **2011**, *33*, 832–847. [[CrossRef](#)]
59. Spiesz, P.R. *Durability of Concrete with Emphasis on Chloride Migration*; Technische Universiteit Eindhoven: Eindhoven, The Netherlands, 2013.
60. Torres Castellanos, N.; Izquierdo García, S.; Torres Agredo, J.; de Gutierrez, R.M. Resistencia a la penetración del ión cloruro y a la carbonatación de concretos adicionados, con un residuo de la industria petroquímica. *Ing. Investig.* **2014**, *34*, 11–16. [[CrossRef](#)]
61. Andrade, C.; D'andrea, R. Electrical resistivity as microstructural parameter for the modelling of service life of reinforced concrete structures. In Proceedings of the 2nd International Symposium on Service Life Design for Infrastructure, Delft, The Netherlands, 4–6 October 2010.
62. Hornbostel, K.; Larsen, C.K.; Geiker, M.R. Relationship between concrete resistivity and corrosion rate—A literature review. *Cem. Concr. Compos.* **2013**, *39*, 60–72. [[CrossRef](#)]
63. Cherif, R.; Hamami, A.A.; Aït-Mokhtar, A.; Meusnier, J.-F. Study of the pore solution and the microstructure of mineral additions blended cement pastes. *Energy Procedia* **2017**, *139*, 584–589. [[CrossRef](#)]



© 2018 by the authors. Licensee MDPI, Basel, Switzerland. This article is an open access article distributed under the terms and conditions of the Creative Commons Attribution (CC BY) license (<http://creativecommons.org/licenses/by/4.0/>).